Quasiequilibria in one-dimensional self-gravitating many-body systems

Toshio Tsuchiya*
National Astronomical Observatory, Mitaka, 181, Japan

Tetsuro Konishi
Department of Physics, Nagoya University, Nagoya, 464-01, Japan

Naoteru Gouda
Department of Earth and Space Science, Osaka University, Toyonaka, 560, Japan
(Received 7 February 1994)

The microscopic dynamics of one-dimensional self-gravitating many-body systems is studied. We examine two courses of the evolution that have the isothermal or stationary water-bag distribution as initial conditions. We investigate the evolution of the systems toward thermal equilibrium. It is found that when the number of degrees of freedom of the system is increased, the water-bag distribution becomes a quasiequilibrium, and the stochasticity of the system reduces. These results suggest that the phase space of the system is effectively not ergodic and the system with large degrees of freedom approaches the near-integrable one.

PACS number(s): 05.45.+b, 98.10.+z, 03.20.+i, 95.10.Ce

I. INTRODUCTION

A self-gravitating many-body system, which contains many particles interacting with mutual gravity, is an idealized model of wide classes of astronomical objects, such as globular clusters, elliptical galaxies, and clusters of galaxy. Dynamics of the system has two characteristic aspects. One is the *microscopic dynamics*, which is concerned with the motions of the individual particles. The other is the *macroscopic dynamics*, which deals with the averaged quantities. Evolution of the real system is determined exactly by the microscopic dynamics. However, the number of the particles contained in the system is so large, e.g., 10^5 for globular clusters and 10^{11} for elliptical galaxies, that we can treat only macroscopic quantities by the statistical method, in practice.

In many cases which are successfully treated by statistical mechanics, which include gas and liquid systems, the particles interact with close neighbors, then the local equilibrium is determined by the state of the neighbors. Thus if the macroscopic quantities are defined by averaging over the scale much larger than the range of the force, their evolution is independent of the microscopic dynamics and is governed only by themselves. In these systems the statistical mechanics is easily applicable.

On the other hand, in the self-gravitating systems, the motions of the individual particles are governed by the summation of the forces from all the other, because the gravity is long range force. Thus, the macroscopic dynamics is not decoupled with the microscopic dynamics. Therefore, we must study how the microscopic dynamics influences the evolution of the macroscopic quantities in the self-gravitating systems.

The microscopic dynamics is described as a trajectory in the Γ space (N-body phase space). If the system has some integrals of motion, the trajectory is confined in the subspace which conserves the integrals. The system is defined as *ergodic* if the time average of any dynamical quantities are equal to the spatial average over the subspace. This subspace is referred to as the ergodic region. In this case, the time average does not depend on the initial condition of the system but only on the integrals, and thus it is time independent. This gives the statistical or microcanonical equilibrium. At the equilibrium, energy is equally distributed to all degrees of freedom, which is called *equipartition.*

The mixing system, which is included in the ergodic system, has the property that a small but finite part of the phase space volume spreads over a whole ergodic region by means of coarse graining. This property is closely related to relaxation of the system, because information of the initial state is lost and the microcanonical equilibrium is realised. Any time-correlation disappears after the trajectory is mixed over the ergodic region [for more detailed reviews, see, e.g., [1,2]]. We refer to the time that mixing is realized as the *microscopic relaxation time.*

Though ergodicity is the fundamental basis of statistical mechanics, not all systems are ergodic. For example, the phase space of a near-integrable Hamiltonian system contains both stochastic region and regular region (tori). A trajectory initially located on a torus stays on it forever. This system is not ergodic over the subspace where the total energy of the system is constant. Furthermore, it is shown that there exist *stagnant layers* around tori and a trajectory in the stagnant layer stays there for a long time [3]. In this system, the trajectory in the stagnant layer moves in the stochastic region after a

*Electronic address: tsuchiya@milano.mtk.nao.ac.jp

long interval of time, and then they could enter another stagnant layer. Thus, in the system, transient stationary states can emerge in some era. We refer to them as *quasiequilibria.*

Lynden-Bell applied the concept of ergodicity to the evolution of elliptical galaxies, and derived the unique equilibrium state [4]. However, observations of elliptical galaxies and numerical simulations show disagreement with the Lynden-Bell distribution [5–7]. In particular, elliptical galaxies are believed to be triaxial in the shape and anisotropic in the velocity dispersion. This stationary state seems to suggest the existence of additional integrals, which conserves the anisotropy, though it is unclear whether the state is a stationary state induced by the additional integrals or only a transient state approaching to the statistical equilibrium. These facts suggest that elliptical galaxies are not ergodic while it is generally believed that the self-gravitating many-body systems are chaotic and so ergodic. So it is very important and interesting to study ergodicity of the self-gravitating many-body systems in order to analyze the present dynamical structures of elliptical galaxies, and, moreover, to examine applicability of usual statistical mechanics to the self-gravitating many-body systems.

To study their ergodicity, we employ one-dimensional system. Because in one-dimension the phase space is compact, which makes the system tractable in considering ergodicity. Another reason is that the force law is very simple and thus the evolution of the system can be followed numerically with a good accuracy by using the "exact code" [8]. Though the force law in one-dimensional system is different from that in the three-dimensional system, we can study the properties induced by long range forces even in the one-dimensional systems.

Hohl [9,8] studied the relaxation time of the one-dimensional system consisting of N identical plane-parallel sheets by using decay of correlation of oscillation of the total kinetic energy. They found that the the time scale is $N^2 t_c$, where t_c is the characteristic time which is approximately the time for a member to traverse the system. However, Wright, Miller, and Stein [10] asserted that some initial states do not approach microcanonical distribution after $2N^2 t_c$. Later it is shown that the weak correlation of density fluctuation persists for times of order $10^3 t_c$ [11]. Thus, the Hohl's conjecture was questioned. In succeeding papers [11–17], it was shown that the evolution of the system greatly depends on the initial condition. Some initial states appear to relax on the time scale of Nt_c, which is much shorter than Hohl's prediction [12,13,18]. Then the complicated features of relaxation in the self-gravitating systems were recognized.

Severne and Luwel [19] suggested that there are three phase in relaxation. If the initial state is far from equilibrium, violent oscillation of mean field gives rise to the violent relaxation [4] for the first several oscillation. After the system almost virialized, remaining small fluctuation of gravitational field causes the change of the individual particle energies. They called this era the collisionless mixing phase. In astrophysics, the evolution in the violent relaxation and the collisionless mixing phase are often referred to dynamical evolution. After that, the collisional relaxation phase takes place, in which the particle interactions tend to drive the system towards the microscopic thermal equilibrium. This is the thermal evolution. Luwel and Severne [14] examined the evolution of the stationary water-bag distribution. They showed that although there is no noticeable evolution in the macroscopic distribution for a long time, the energy of individual particles fluctuates broadly in the energy space. They concluded that it is the collisionless mixing. In the present paper, we found the collisional relaxation occurs in the water-bag distribution on the time scale $10^6 t_c$, which is much longer than the simulation time of Luwel and Severne.

While the above studies are concerned with the evolution of the macroscopic quantities, the microscopic dynamics, especially the ergodicity of the system also has been studied by some authors. For small N ($N \leq 10$) it is shown that the stochasticity of the system is strengthened as N increases [20–22]. Most of the phase space is covered by stochastic orbits, but Reidl and Miller [23] found an existing region which is covered by stable orbits with zero Lyapunov exponents. Thus such small N systems are not exactly ergodic.

Reidl and Miller [23] also showed that for $N = 11$ the convergence of Lyapunov exponents occurs in a very long time scale ($\sim 10^7 t_c$). This suggests the segmentation of the phase space which occurs for $N \leq 10$ disappears and the system is ergodic.

In this paper, we are interested in the relation between the microscopic dynamics and the macroscopic evolution in larger N. In order to get more information of microscopic dynamics, we have investigated the time correlation of the fluctuation of the individual particle energies, the equipartition of the individual particle energies, and the convergence of the maximum Lyapunov exponent. In general, the motion in an ergodic region shows fast decay of correlation. On the other hand, in the near integrable Hamilton system an essential feature of the diffusion process (including the Arnold diffusion) is the appearance of long time tails of the correlation or the enhancement of the diffusion mode with the zero frequency, e.g., the power spectrum density (PSD) function $S(f)$ satisfies,

$$S(f) \sim f^{-\nu} \quad (f \ll 1), \tag{1}$$

where f stands for the frequency and ν a positive constant ($2 > \nu > 1$) [3,24]. Therefore the time correlation or the PSD is a good tool to understand the ergodicity of the phase space, besides the equipartition of the energies and the convergence of the maximum Lyapunov exponents.

In Sec. II we describe the model and the initial conditions. Three quantities which we employ to analyze the system are explained in Sec. III and results of the numerical simulations are given in Sec. IV. We devote Sec. V to the conclusions and discussions.

II. DESCRIPTION OF THE MODEL

The one-dimensional self-gravitating system consists of N identical mass sheets, each of uniform mass density

and infinite in extent in the (y, z) plane. We call the sheet a particle in this paper. The particles are free to move along x axis and accelerate as a result of their mutual gravitational attraction. The Hamiltonian of the system is given by

$$H = \frac{m}{2}\sum_{i=1}^{N} v_i^2 + (2\pi G m^2)\sum_{i<j}|x_j - x_i|, \tag{2}$$

where m, v_i, and x_i are the mass (surface density), velocity, and position of the ith particle, respectively. Since the gravitational field is uniform, the individual particles moves parabolically, until they intersect with the neighbors. Thus, the evolution of the system can be followed by connecting the parabolic motions. When an encounter occurs between two particles, they pass freely through each other.

Our code is the application of that for one-dimensional sheet plasma [25] to the self-gravitating systems, which is very similar to the "new exact code" referred in Ref. [19], but the exchange of particles at an encounter is arranged by the heap sort algorithm. During the integration, time is measured in the unit

$$t_c = (4\pi G\rho_{\rm av})^{-1/2}, \tag{3}$$

where $\rho_{\rm av}$ is the mass divided by the width of the distribution at the initial time.

All calculations were performed in double precision (16 significant figures) on DEC station 3000AXP and SONY NEWS 5000 computers. The total energy was conserved to better than one part in 10^{13}.

We examined two courses of evolution, IT and WB, which begin with the isothermal and water-bag distributions as their initial condition, respectively. In the water-bag distribution, all particles are randomly distributed in a rectangle region in the μ space to form a uniform averaged phase density (Fig. 1). This is not a exact stationary solution of the collisionless Boltzmann-Poisson equations because the shape is a rectangle, but the difference is very small and then after several oscillations it is transformed into the stationary water-bag configuration. The isothermal distribution is given by

$$\theta(\eta) = \pi^{-1/2}\exp(-\eta^2) \quad \text{(velocity)}, \tag{4}$$

$$\rho(\xi) = \frac{1}{2}\mathrm{sech}^2\xi \quad \text{(position)}, \tag{5}$$

where

$$\eta = (v/2)(3M/E)^{1/2}, \tag{6}$$

and

$$\xi = (3\pi GM^2/2E)x, \tag{7}$$

M and E represent the total system mass and total energy, respectively (Fig. 2). It is a stationary solution of the collisionless Boltzmann-Poisson equations. In all our simulations, the total mass and energy set to 1 and 1/4, respectively. The typical period of oscillation of a particle is $2\pi t_c$.

We choose the initial distributions which are dynamically stable, because our studies are concentrated on the thermal evolution (collisional relaxation) of the system. If the system is ergodic, IT and WB should coincide after the relaxation time. Therefore we compare the behaviours of IT and WB for a long time.

III. ANALYSES

A. Equipartition

The specific energy (energy per unit mass) $\varepsilon_i(t)$ of ith particle is given by

$$\varepsilon_i(t) = \frac{1}{2}v_i^2(t) + 2\pi G m\sum_{j=1}^{N}|x_j(t) - x_i(t)|. \tag{8}$$

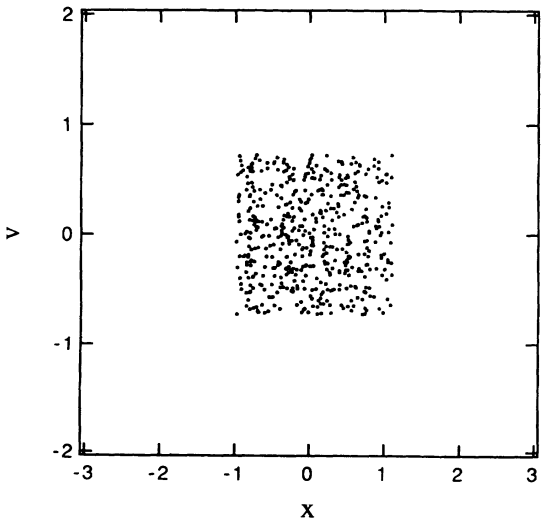

FIG. 1. The water-bag initial distribution in μ space.

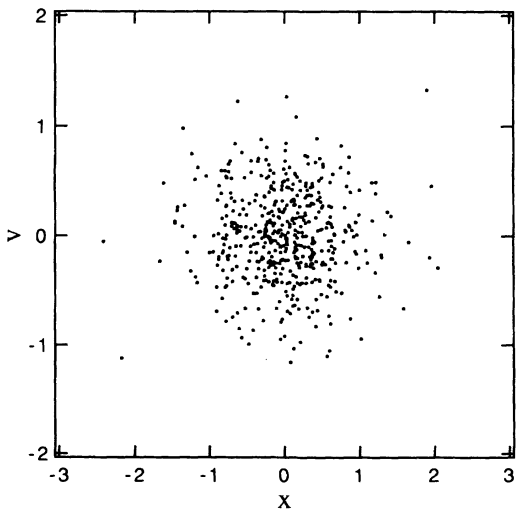

FIG. 2. The isothermal initial distribution in μ space.

If the evolution of the system is ergodic in the Γ space, the long time average of the specific energy takes a unique value for all i, i.e.,

$$\overline{\varepsilon_i} \equiv \lim_{T\to\infty} \frac{1}{T}\int_0^T \varepsilon_i(t)dt = \varepsilon_0 \equiv 5E/3. \tag{9}$$

The degree of the deviation from the equipartition is measured by the quantity,

$$\Delta(t) \equiv \varepsilon_0^{-1}\sqrt{\frac{1}{N}\sum_{i=1}^{N}[\overline{\varepsilon_i}(t) - \varepsilon_0]^2}, \tag{10}$$

where $\overline{\varepsilon_i}(t)$ is the averaged value until t. In the numerical scheme, $\varepsilon_i(t)$s are sampled at every $\Delta t = 0.781\,25t_c$, and the average is defined simply by the summation of the samples divided by the number of the samples.

If the system is ergodic and has a finite correlation time (the relaxation time), it behaves like a random number from Markovian process and we can estimate the temporal evolution of $\Delta(t)$. In this case, a trajectory in the Γ space visits almost every point in the ergodic region, thus, the individual particle energy relaxes to equilibrium value and $\Delta(t)$ decreases as $t^{-1/2}$ for the time longer than the relaxation time, according to the central limit theorem. Therefore, the evolution of $\Delta(t)$ is a good tool to understand the relaxation property of the system.

The initial value of the deviation from the equipartition, $\Delta(0)$, depends on the initial distribution. Figure 3 shows the cumulative distribution of the specific energy, $\hat{\nu}(\varepsilon)$, which is defined by

$$\hat{\nu}(\varepsilon) \equiv (1/N)N(\varepsilon_i \le \varepsilon), \tag{11}$$

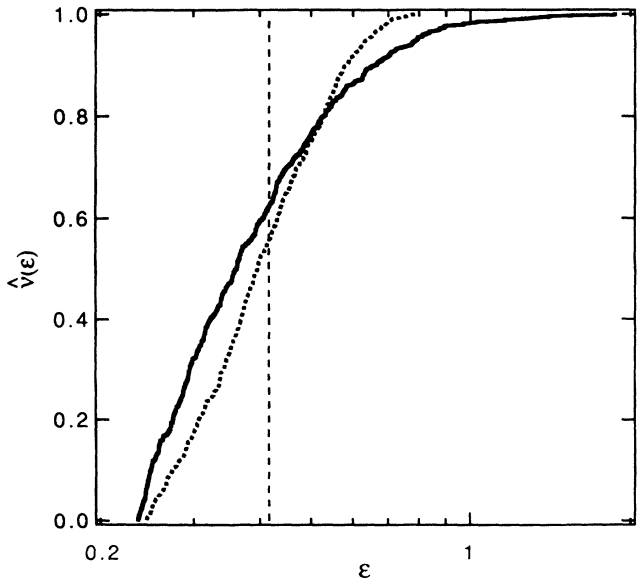

FIG. 3. The cumulative specific energy distribution of the isothermal (solid line) and water-bag (dashed line) distribution for $N = 512$. The dotted line indicates the energy at equipartition.

where $N(\varepsilon_i \le \varepsilon)$ is the number of particles with $\varepsilon_i \le \varepsilon$. The isothermal and water-bag distribution are represented by the solid and dashed lines, respectively. Also the energy at the equipartition, ε_0, is shown by dotted line. Since the isothermal distribution spreads wider in the energy space than the water-bag, $\Delta(0)$ of the isothermal distribution is larger than that of the water-bag distribution.

B. Power spectrum density

The power spectrum density (PSD) $S(f)$ is given by

$$S(f) \equiv (1/N)\sum_{i=1}^{N}|C_i(f)|^2, \tag{12}$$

where $C_i(f)$ is Fourier transform of $\varepsilon_i(t)$, i.e.,

$$\varepsilon_i(t) = \int C_i(f)\mathrm{e}^{-2\pi i f t}df. \tag{13}$$

The PSD, on the other hand, is the Fourier transform of the autocorrelation function, thus the long time correlation gives rise to a peak at small f. In order to obtain PSD numerically, a sequence of "locally averaged" energy $\{\langle\varepsilon\rangle(t_1 = T_0/n), \langle\varepsilon\rangle(t_2 = 2T_0/n), \ldots, \langle\varepsilon\rangle(t_n = T_0)\}$ is sampled, where

$$\langle\varepsilon\rangle_i(t_j) = \frac{1}{t_1}\int_{t_{j-1}}^{t_j}\varepsilon_i(t)dt. \tag{14}$$

The maximum integration time T_0 determines the minimum frequency $f_{\min} = 1/T_0$, and the interval of sampling determines the maximum frequency $f_{\max}$. This local averaging suppresses the frequency modes higher than $f_{\max}$ thus it prevents the higher frequency modes from falling into the interval of $f \le f_{\max}$ [26]. The procedure of the local averaging, Eq. (14), is the same as that described in the previous section. We integrated the motion to $T_0 = 10^7 t_c$ for N =32 and 128, hence $f_{\min} = 10^{-7}t_c^{-1}$. The number of samples n is limited to 256 due to the computer's ability, hence $f_{\max} = 2.56 \times 10^{-5}t_c^{-1}$. In order to obtain higher f, we gathered n samples with shorter time interval, $\{\langle\varepsilon_i\rangle(T_0/10n), \langle\varepsilon_i\rangle(T_0/10n), \langle\varepsilon_i\rangle(2T_0/10n), \ldots, \langle\varepsilon_i\rangle(T_0/10)\}$, which covers the range of the frequency from $10^{-6}t_c^{-1}$ to $2.56 \times 10^{-4}t_c^{-1}$. If the amplitude of oscillation with the frequency $10^{-6}t_c^{-1} \le f \le 2.56 \times 10^{-5}t_c^{-1}$ for $t \ge 10^6 t_c$ is the same as during $t \le 10^6 t_c$, two $S(f)$ merge into one curve. In this way, we extended the range of the frequency beyond $10^{-2}t_c^{-1}$. The system with $N = 128$ is the exception that makes the values of $S(f)$ of $T_0 = 10^7 t_c$ and $T_0 \le 10^6 t_c$, for $10^6 t_c^{-1} \le f \le 2.56\times10^{-5}t_c^{-1}$ different (Fig. 4). This is discussed in the next section.

Since the PSD is the Fourier transform of the autocorrelation function,

$$\xi_\varepsilon(t) \equiv \int \varepsilon(t+t')\varepsilon(t')dt', \tag{15}$$

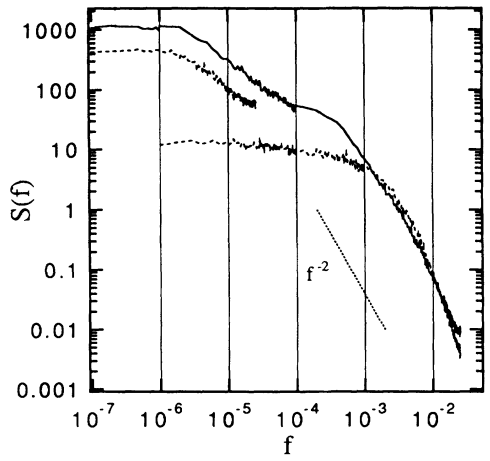

FIG. 4. Same as Fig. 6, but for $N = 128$.

we can find the time scale on which the correlation decays. For example, the Brownian motion, $u(t)$, subjected by the Langevin equation,

$$\frac{du}{dt} + \gamma u = R(t), \tag{16}$$

where γ is the friction coefficient and $R(t)$ is a random force (white noise), gives the PSD of the Lorentz distribution,

$$S(f) \propto \frac{1}{f^2 + \gamma^2}. \tag{17}$$

For $f \gg \gamma$, $S(f) \propto f^{-2}$, which describes the short time scale nature of the system. In this phase, the random force $R(t)$ is dominated and the dispersion $\langle [u(t) - u(0)]^2 \rangle$ increases proportional to t. In other words, it is the diffusion phase from its initial value. On the other hand, for $f \ll \gamma$, $S(f)$ is constant. Thus any correlation disappears in the time scale γ^{-1}, and then the fluctuation becomes like a thermal noise. Since this time scale is closely related to the relaxation time, the PSD gives us complemental information about the mixing property of the system.

We should mention more about the PSD with a peak or divergence as f goes to zero, e.g., $S(f) \propto f^{-1}$, which means the existence of a long time correlation. Such a PSD is often observed in a near-integrable system. In the system, the phase space is divided into stochastic region and regular region (tori). The well known Arnold diffusion states that it takes a long time for a trajectory to travel across the web of the tori. This slow diffusion gives rise to a long time correlation [3].

C. Lyapunov exponent

The evolution of the system can be described as a trajectory in the Γ space. The Lyapunov exponents of a given trajectory characterized the mean exponential rate of divergence of trajectories surrounding it (a general discussion of the Lyapunov exponents is provided by Lichtenberg and Lieberman [2]).

The maximum Lyapunov exponent is defined as

$$\lambda = \lim_{\substack{d(0)\to 0 \\ t\to\infty}} \frac{1}{t} \ln \frac{d(t)}{d(0)}, \tag{18}$$

where $d(t)$ and $d(0)$ are the separations in the Γ space between two nearby orbits at times t and 0, respectively. The numerical procedure follows mostly Shimada and Nagashima [27], where $d(t)$ is determined by the linearized equations of motion:

$$\Delta \dot{x}_i = \Delta v_i, \tag{19}$$

$$\Delta \dot{v}_i = -4\pi G m \sum_{j=1}^{N} (\Delta x_i - \Delta x_j)\delta(x_i - x_j), \tag{20}$$

$$d \equiv \sqrt{\sum_{j=1}^{N} (\Delta x_i^2 + \Delta v_i^2)}, \tag{21}$$

where Δx_i and Δv_i are the first order deviation of the position and velocity. Since $d(t)$ diverges exponentially, when the separation d becomes 10^5 times the initial value, the separation is rescaled to $d(0)$.

The linearized equation (20) contains the δ functions, but is is not harmful. Because the δ function comes from the singularity in time (at the intersection of sheets), then displacement at a given time is a smooth function of the positions and the velocities. To make sure, we calculated the Lyapunov exponents by tracing two nearby orbits, which is used, e.g., in Ref. [18], and we got the same value as the one we obtain by linearization.

The Lyapunov exponent is originally defined by the limit of infinite t, but here we use "time-dependent Lyapunov exponent" defined by

$$\lambda(t) = \frac{1}{t} \ln \frac{d(t)}{d(0)}. \tag{22}$$

If the system is mixing, the time average becomes roughly the same as the space average over ergodic region, in the relaxation time. Thus the convergence of $\lambda(t)$ gives another measure of relaxation.

IV. RESULTS

A. $N = 32$

Figure 5 shows the time evolution of the deviation from the equipartition, $\Delta(t)$ (bold lines) and the Lyapunov exponents, $\lambda(t)$ (light lines). The PSD, $S(f)$, are shown in Fig. 6. The curves of IT and WB are represented by solid and dashed lines, respectively.

The features of the curves are not so simple as we expected in the previous section. $\Delta(t)$ begins to decrease at $t \sim 3 \times 10^3 t_c$, but does not show monotonic decrease like $t^{-1/2}$. From $t \sim 3 \times 10^3 t_c$, $\Delta(t)$ of IT and WB coincide, but at $t \sim 10^4 t_c$, IT begins to increase again and the difference between IT and WB lasts until $t \sim 3 \times 10^6 t_c$.

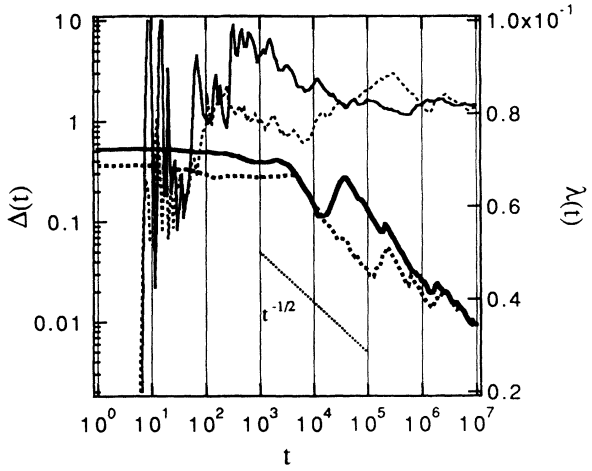

FIG. 5. Evolution of the deviation from the equipartition, $\Delta(t)$ (bold lines), and the maximum Lyapunov exponent, $\lambda(t)$ (light lines) for $N = 32$. The solid and dashed lines represents IT and WB, respectively. The unit of time is t_c.

After that, though the range of t is not so long, $\Delta(t)$ seems to decrease as $t^{-1/2}$. At this time, $t \sim 3 \times 10^6 t_c$, also the convergence of $\lambda(t)$ becomes quite clear. From the PSD (Fig. 6), it is found that $S(f)$ is constant for $f \ll 10^{-5} t_c^{-1}$, which gives the time scale of disappearance of correlation of $t \sim 10^5 t_c$. Therefore, it is probable that the system relaxes on this time, $t \sim 10^6 t_c$.

From Fig. 5, there seems to exist another time scale, $t \sim 10^3 t_c$, at which $\Delta(t)$ begins to decrease. For shorter period, $t \ll 10^3 t_c$, the PSD indicates that the variation of $\varepsilon_i(t)$ is well approximated by the random walk because $S(f) \propto f^{-2}$. For $t \gtrsim 3 \times 10^3 t_c$, the trajectory in the Γ space travels farther so that the individual particle energies vary widely over the energy space. However, the long time correlation seems to last for several $10^4 t_c$, because $\Delta(t)$ does not decrease monotonically like $t^{-1/2}$ but sometimes decrease more rapidly and sometimes increases. Also, convergence of $\lambda(t)$ is not good.

From the facts that the Lyapunov exponents obtained for different initial conditions tend to converge to the same value, it is speculated that the system has ergodic property and an orbit covers the whole phase space. However, it is interesting that the diffusion in the phase space is different from that of the Markovian random number. The complicated behavior of $\Delta(t)$ suggest a long time correlation of about $t \sim 10^5 t_c$.

B. N=128

Figures 7 and 4 are the same as Figs. 5 and 6, but for $N = 128$. The PSD for WB is that $S(f)$ is separated into two part, $10^{-7} t_c^{-1} \leq f \leq 2.56 \times 10^{-5} t_c^{-1}$ and $10^{-6} t_c^{-1} \leq f \leq 2.56 \times 10^{-2} t_c^{-1}$. The former is calculated from the sample of $T_0 = 10^7 t_c$ and $n = 256$ (see Sec. III B). The other is calculated from that of $T_0 \leq 10^6 t_c$, thus this part does not contain the behavior during $10^6 t_c \leq t$. The difference between the two means that evolution with a period $10^6 t_c$ later than $t = 10^6 t_c$ is different from that of $0 \leq t \leq 10^6 t_c$. The transition of state at $t \sim 10^6 t_c$ is found in Fig. 7. $\Delta(t)$ of WB decreases as $t^{-1/2}$ until $t \leq 10^6 t_c$ and then suddenly increases to approach to IT. Also $\lambda(t)$ shows the transition at $t \sim 2 \times 10^6 t_c$. After that $\Delta(t)$ and $\lambda(t)$ of WB show a tendency to approach to that of IT. Therefore the system is expected to relax on the time scale of $10^7 t_c$.

Another interesting feature of this system is the behavior of WB for $t < 10^6 t_c$. $\Delta(t)$ shows a good agreement with $t^{-1/2}$ from $t \sim 10^2 t_c$, and $\lambda(t)$ converges to the local value, 5.5×10^{-2}, while that of IT converges to 6.2×10^{-2}. Furthermore, $S(f)$ calculated from the sample of $T_0 \leq 10^6 t_c$ shows almost flat spectrum for $f < 10^{-3} t_c^{-1}$. These features indicate that WB relaxes in $t \sim 10^3 t_c$ to a quasiequilibrium which lasts until $t \sim 10^6 t_c$. Figure 8 shows the cumulative energy distribution, $\hat{\nu}(\varepsilon)$, of IT at the beginning, $t = 0$, (solid line), WB at the beginning (dashed line), and WB at $t = 10^6 t_c$ (dotted line). The distribution of WB at $t = 10^6 t_c$ is very close to the initial distribution compared with the

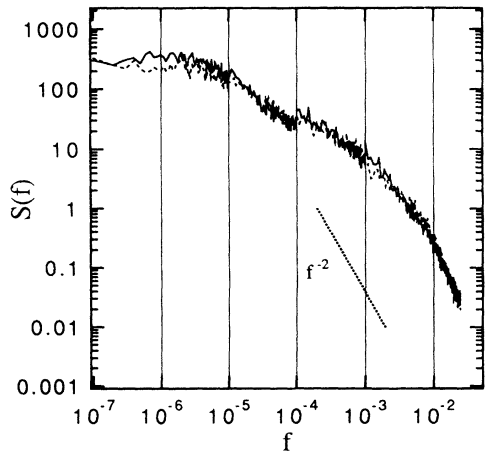

FIG. 6. Power spectrum densities of IT (solid line) and WB (dashed line) for $N = 32$. The unit of frequency is t_c^{-1}.

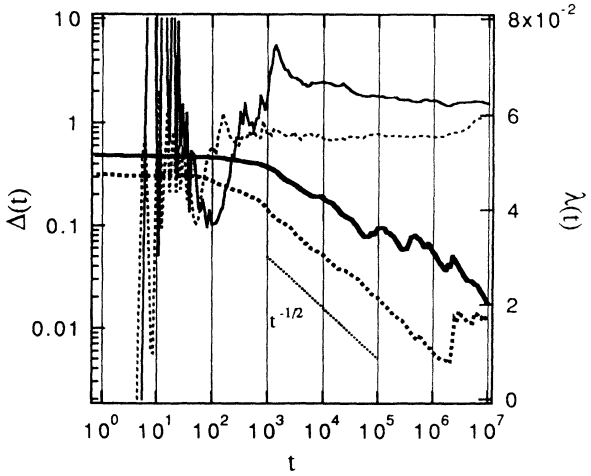

FIG. 7. Same as Fig. 5, but for $N = 128$.

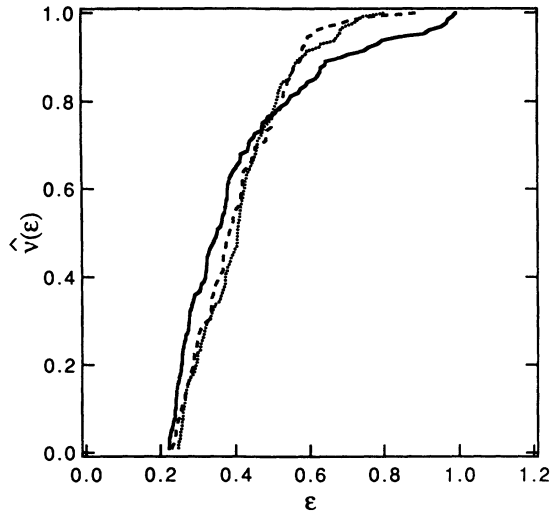

FIG. 8. Cumulative energy distributions, $\hat{\nu}(\varepsilon)$, of IT at the beginning, $t = 0$ (solid line), WB at the beginning (dashed line), and WB at $t = 10^6 t_c$ (dotted line).

isothermal distribution. Therefore the quasiequilibrium has, in fact, the water-bag distribution. On the other hand, the difference between IT and WB disappears after the transition. Figure 9 shows $\hat{\nu}(\varepsilon)$ of IT (solid line) and WB (dashed line) at $t = 10^7 t_c$.

The evolution of IT is similar to that of $N = 32$. There is a long time correlation, which is found from the evolution of $\Delta(t)$ and $\lambda(t)$. Especially for $N = 128$, PSD shows clear bend at $f = 2 \times 10^{-4} t_c^{-1}$, and the power of f for $10^{-6} t_c^{-1} < f < 10^{-4} t_c^{-1}$ is less steep than f^{-2}. This smaller power means slower diffusion than the random walk diffusion. The similar feature of PSD can be found in that of WB for $f \leq 2.56 \times 10^5 t_c^{-1}$. This is the transition phase from the water-bag distribution to the isothermal one. Thus in this transition phase the diffusion the phase space is slower than in the quasiequilibrium.

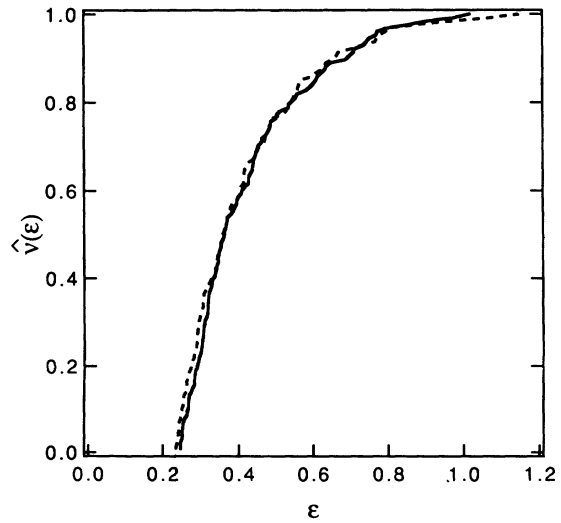

FIG. 9. Cumulative energy distributions, $\hat{\nu}(\varepsilon)$, of IT (solid line) and WB (dashed line) at $t = 10^7 t_c$.

C. $N = 512$

Figures 10 and 11 are the same as Figs. 5 and 6 but for $N = 512$, respectively.

The PSD indicates that the behavior in a shorter time scale than $10^3 t_c$ is the same for IT and WB. It is the diffusion process of the individual particle energy from its initial value.

Since the integration time is limited to $10^6 t_c$ from the constraint of computer's ability, the transition of WB from the water bag to the isothermal distribution, which is expected to occur at later than $10^6 t_c$, is not observed. The behavior of WB for $t \leq 10^6 t_c$ is quite similar to that for $N = 128$. Thus water-bag distribution is one of quasiequilibrium and the relaxation time to the quasiequilibrium is about several $10^3 t_c$.

Increasing the number of the particles for IT strengthens the property that disappearance of time-correlation which is found by the bend of the PSD occurs later for the larger N. In fact, the frequency at which the feature of PSD changes from flat to inclined is $10^{-5} t_c^{-1}$ for $N = 32$ and $10^{-6} t_c^{-1}$ for $N = 128$. Together with the fact that $\Delta(t)$ does not decrease as $t^{-1/2}$, we found that the relaxation time, at which the trajectory covers almost whole ergodic region, becomes longer for larger N.

V. CONCLUSIONS AND DISCUSSIONS

We performed N-body simulations of the evolution of one-dimensional self-gravitating systems for different N. We examined two courses of evolution, IT and WB, which have the initial distributions of the isothermal and water bag, respectively. We obtained the following lines of conclusion.

(1) These systems relax to the isothermal distribution. The time at which the difference between IT and WB disappears is about $10^6 t_c$ for $N = 32$, $10^6 t_c$ for $N = 128$, and longer than $10^6 t_c$ for $N = 512$.

(2) As N increases, the water-bag distribution becomes

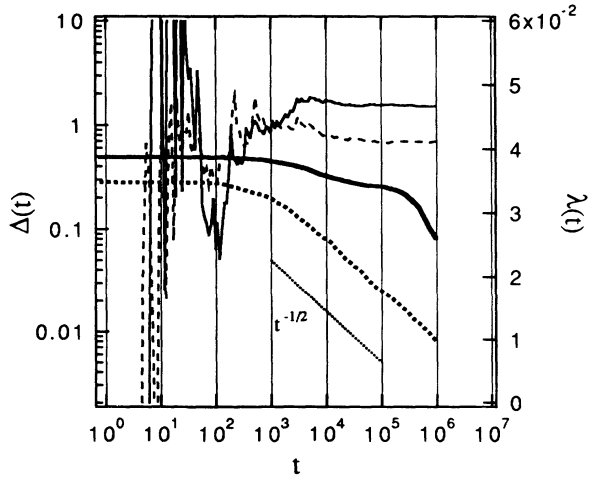

FIG. 10. Same as Fig. 5, but for $N = 512$.

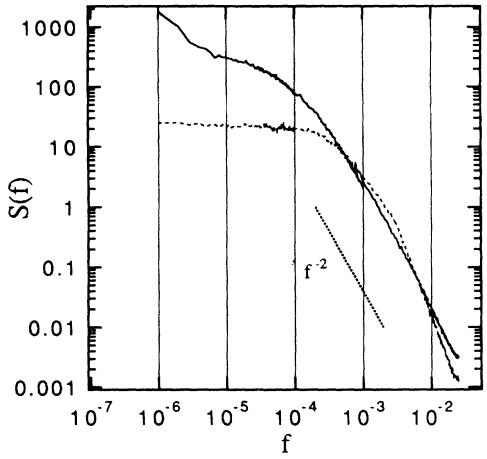

FIG. 11. Same as Fig. 6, but for $N = 512$.

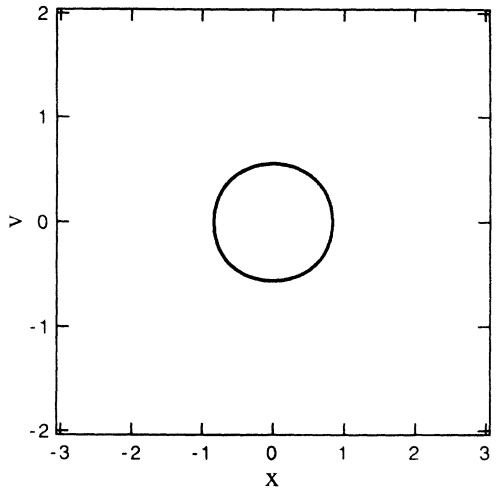

FIG. 12. Distribution of particle in a stationary solution of collisionless Boltzmann-Poisson equations. All the particles have the same energy.

a quasiequilibrium, which yields ergodic properties apparently. The microscopic relaxation time of the water bag, at which the time correlation disappears, is $10^3 t_c$ for $N = 128$ and $10^4 t_c$ for $N = 512$. The water-bag distribution lasts stably for a period orders of magnitude longer time than the time that the correlation disappears.

(3) Since the isothermal distribution is the microcanonical equilibrium, IT shows no evolution macroscopically. As one can see in the figures of PSD, the microscopic relaxation time is, however, much longer than that of the water-bag quasi-equilibrium. For $N = 32$, the microscopic relaxation time is about $10^5 t_c$ and $10^6 t_c$ for $N = 128$. For $N = 512$, we did not observe the microscopic relaxation in $10^6 t_c$. The transition of the water bag to the isothermal distribution occurs in the same time scale.

(4) Convergence of the maximum time-dependent Lyapunov exponents to the different values for IT and WB indicates that the phase space is separated into at least two ergodiclike regions which give the quasiequilibria.

In the limit of $N \to \infty$ the evolution of the system, both the isothermal and water-bag distribution are the stationary solution of the collisionless Boltzmann-Poisson equations. The distribution function which depends only on the individual particle energy is always the stationary solution of the collisionless Boltzmann equation. Among these solutions many satisfy the Poisson equation, so many classes of analytic stationary solutions for the collisionless Boltzmann-Poisson equations exist. These solutions are expected to be also quasiequilibria, and they should depend on the initial condition. In fact, we have examined another initial condition, in which all particles have the same energy. The distribution of particles is shown in Fig. 12. Since this distribution is unstable, the ellipse in the phase space is broken rapidly, then the system approaches not to the isothermal distribution but to the water-bag distribution. So in this case, the final results are similar to the one for WB mentioned before. Furthermore, we are presently studying the dependence of the initial condition in more detail. The result will be described in the succeeding paper.

After a very long time [e.g., ($t \gg 10^6 t_c$) in Fig. 7] the system appears to be ergodic. However, from the above facts, it is obvious that in view in shorter time ($t < 10^6 t_c$) the ergodicity is effectively broken. This means that there are many regions in the phase space, in which trajectories are confined for a long time and give the quasiequilibria. In those regions trajectories show normal diffusion like the random walk, and the trajectlies covers the whole subregions like ergodic systems. We call this era "quasiequilibrium." The trajectories temporaly trapped in the subregions eventually cover the whole phase space. However, during transition from a quasiequilibrium to the true equilibrium the diffusion of the trajectories exhibit a long time correlation.

Though the origin of the substructures is not clear, we have a speculation that tori play an important role. This idea conflicts with the usual idea that chaos is strengthened as the number of degrees of freedom increases, thus the system approaches to ergodic. The latter idea is supported by some numerical results, in which the volume of the Kolmogorov-Arnold-Moser tori is reduced as the number of degrees of freedom increases [28,29]. However, we believe our idea, because of the following reasons: in the limit of $N \to \infty$, the distribution function which depends only on the individual particle energy is alway the stationary solution of the collisionless Boltzmann equation. These solutions form tori because all phase elements in the phase space (i.e., all degrees of freedom) conserves their energy, and the motion which has the same number of integrals of motion as the degree of freedom is a torus. Thus, in the limit the system contains many tori, which seem to produce the multiergodicity [3]. The other reason is that, in fact, chaos is getting weaker as N increases. Figure 13 shows the converged value of the maximum time-dependent Lyapunov exponents of IT and WB for various N. That of IT decreases as $N^{-1/5}$ and of WB as $N^{-1/4}$. This fact suggests that the system approaches to near-integrable system as N increases.

The property that chaos becomes weaker as the number of degrees of freedom of the system increases seems

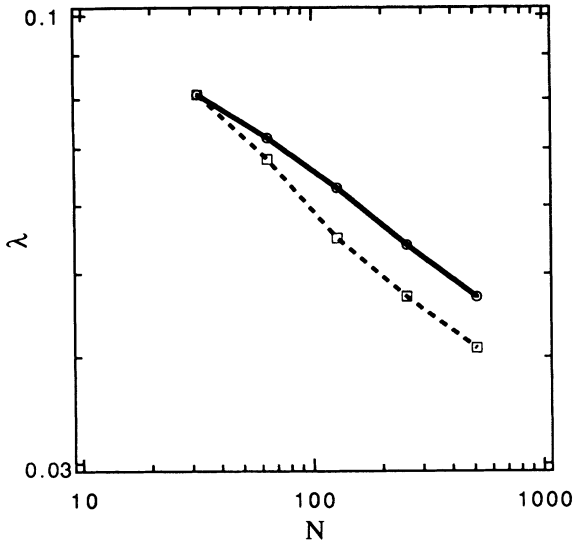

FIG. 13. The maximum Lyapunov exponents of IT (solid line) and WB (dashed line) after convergence.

due to the long range force, because the force acting on a particle is the summation of the force of all the others, thus, the effect of close encounter, which is usually believed to be the origin of chaos, becomes weaker as the system population increases. The results for $N \leq 10$ that the stochasticity of the systems are strengthened [20–22] seem to be due to the small number of particles in the system. In such systems, the properties of the long range force are not prominent. Thus, it is inferred that there exists the number of degrees of freedom which maximizes the stochasticity of the system between 10 and 30.

In the three-dimensional system, the properties described above are expected to hold, because the force is also long range. In fact, elliptical galaxies have the stationary state which is triaxial in shape and anisotropic in the velocity dispersion. Also, the stationary states depend on the initial conditions [5,6]. This state is completely different from what Lynden-Bell predicted by using ergodic hypotheses [4]. This state can be explained as the quasiequilibrium mentioned in this paper.

ACKNOWLEDGMENTS

It is a pleasure to thank Y. Aizawa and S. Takesue for many stimulating discussions, and to thank K. Kitahara for introducing us to the numerical method. A part of computations was carried out on DEC station 3000AXP computer of Cosmic-Ray group, Department of Physics, Kyoto University.

[1] V. I. Arnold and A. Avez, *Ergodic Problems of Classical Mechanics* (Benjamin, New York, 1968).
[2] A. J. Lichtenberg and M. Lieberman, *Regular and Chaotic Dynamics* (Springer-Verlag, New York, 1983).
[3] Y. Aizawa *et al.*, Prog. Theor. Phys. Suppl. **98**, 36 (1989).
[4] D. Lynden-Bell, Mon. Not. R. Astron. Soc. **136**, 101 (1967).
[5] T. de Zeeuw and M. Franx, Annu. Rev. Astron. Astrophys. **29**, 239 (1991).
[6] Y. Funato, J. Makino, and T. Ebisuzaki, Publ. Astron. Soc. Jpn. **44**, 291 (1992).
[7] T. Yamashiro, N. Gouda, and M. Sakagami, Prog. Theor. Phys. **88**, 269 (1992).
[8] F. Hohl and M. R. Feix, Astrophys. J. **147**, 1164 (1967).
[9] F. Hohl and D. T. Broaddus, Phys. Lett. A **25**, 713 (1967).
[10] H. L. Wright, B. N. Miller, and W. E. Stein, Astrophys. Space Sci. **84**, 421 (1982).
[11] B. N. Miller and C. J. Reidl, Jr., Astrophys. J. **348**, 203 (1990).
[12] M. Luwel, G. Severne, and P. J. Rousseeuw, Astrophys. Space Sci. **100**, 261 (1984).
[13] G. Severne, M. Luwel, and P. J. Rousseeuw, Astron. Astrophys. **138**, 365 (1984).
[14] M. Luwel and G. Severne, Astron. Astrophys. **152**, 305 (1985).
[15] C. J. Reidl, Jr. and B. N. Miller, Astrophys. J. **318**, 248 (1987).
[16] C. J. Reidl, Jr. and B. N. Miller, Astrophys. J. **332**, 619 (1988).
[17] C. J. Reidl, Jr. and B. N. Miller, Astrophys. J. **371**, 260 (1991).
[18] C. J. Reidl, Jr. and B. N. Miller, Phys. Rev. A **46**, 837 (1992).
[19] G. Severne and M. Luwel, Astrophys. Space Sci. **122**, 299 (1986).
[20] C. Froeschlé and J.-P. Scheidecker, Phys. Rev. A **12**, 2137 (1975).
[21] G. Benettin, C. Froeschle, and J. P. Scheidecker, Phys. Rev. A **19**, 2454 (1979).
[22] H. L. Wright and B. N. Miller, Phys. Rev. A **29**, 1411 (1984).
[23] C. J. Reidl, Jr. and B. N. Miller, Phys. Rev. E **48**, 4250 (1993).
[24] A. Zacherl, T. Geisel, J. Nierwetberg, and G. Radons, Phys. Lett. A **114**, 317 (1986).
[25] Y. Mitsumori, Master's thesis, Tokyo Institute of Technology, 1992.
[26] W. H. Press, B. P. Flannery, S. A. Teukolsky, and W. T. Vetterling, *Numerical Recipes* (Cambridge University Press, Cambridge, 1988).
[27] I. Shimada and T. Nagashima, Prog. Theor. Phys. **61**, 1605 (1979).
[28] G. Gallavotti, in *Scaling and Self-Similarity in Physics*, edited by J. Fröhlich (Birkhäuser, Boston, 1983), p. 359.
[29] T. Konishi, Prog. Theor. Phys. Suppl. **98**, 19 (1989).